The 2009 IEEE/RSJ International Conference on
Intelligent Robots and Systems
October 11-15, 2009 St. Louis, USA

Size-Dependent Microparticle Filtration Using Magnetically Driven Microtool for Producing Gel-Microtool

Benoît Chapurlat, Hisataka Maruyama, YokoYamanishi, Kyosuke Kotani and Fumihito Arai, Member, IEEE

Abstract— **In this study, we successfully produced a functional microtool made of gel microbeads using size-dependent microparticle classification. Gel microbeads are made by salting-out hydrophilic photo-crosslinkable resin ENT-3400. These gel microbeads were separated according to their size using microfilters made of polydimethylsiloxane (PDMS). The first filter is a row of fluidic microchannels that block microbeads with a size greater than the channel's width. Another filtration method has been examined using a magnetically driven microtool (MMT) to separate the beads using the centrifugal force created by this MMT actuated with a DC motor. Separated gel microbeads were recovered after filtration and used to fabricate functional microtools, for example, a tether-shaped gel tool, by contact with other gel microbeads under UV illumination. The produced gel tool is manipulated using optical tweezers in a microchip. We successfully achieved size-dependent separation of gel microbeads and production of a tether-shaped gel tool.**

I. Introduction

Recently, on-chip experimentation has become important for the investigation of unknown properties of particles such as cells and microorganisms. To analyze the detailed properties of a cell, it is necessary to achieve precise manipulation, such as positioning and attitude control, of a target a few micrometers or less in size. Optical tweezers are suitable for selective manipulation in microchips; however, they may damage the target in case of direct manipulation. Therefore, our group proposed indirect laser manipulation methods with functional microtools for on-chip experiments. In previous studies, we developed gel tools made of a hydrophilic photo-crosslinkable resin and achieved cell manipulation, cell immobilization, and local measurement of parameters such as pH and temperature inside a microchip [1, 2]. Nevertheless, it is not easy to manipulate cells stably using conventional sphere-shaped gel tools. To improve the operability of cell experiments, functional microtools with a complicated structure, such as the tether and microhand presented in Fig. 1, and with fine controllability by optical tweezers are demanded.

We proposed a functional microtool made by connecting spherical gel microbeads, because a sphere shape is best for stable manipulation using optical tweezers. Gel microbeads are made by stirring a mixture of ENT-3400 (Kansai Paint Co. Ltd.) and 8.0 wt% phosphate dipotassium salt solution. The gel microbead generation process forms beads with a wide variety of diameters in the range of a few micrometers usually from 1 μm or less up to 20 μm. To produce the microtool, it is necessary to prepare gel microbeads of a uniform size. Few methods are available to control bead formation [3, 4, 5, 6, and 7] so that they would all have the desired dimensions. It is possible to isolate a few beads and select a particular size using optical tweezers [8, 9]. Of course, this is tedious work, as it involves only human judgment, and would take too much time to provide enough beads for multiple measurements. For these reasons, we intend to design a chip that would allow us to automatically sort the beads and obtain large quantities of gel microbeads that could be stocked and used with any device that needs local parameter measurements. In this presentation, we aim at size-dependent particle classification using microfilters and the production of a tether-shaped gel tool.

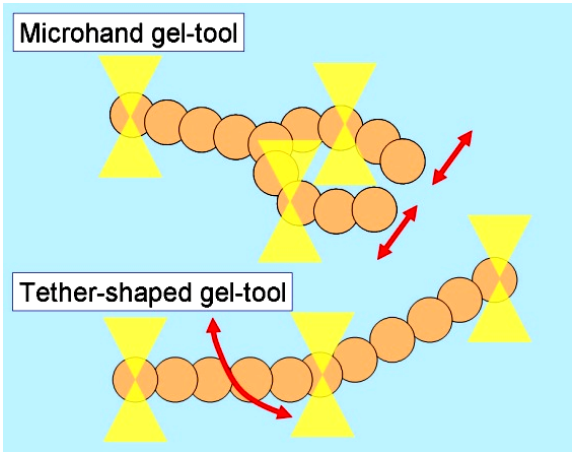

Fig. 1. Schematics of functional-shaped gel tools made by connecting gel microbeads.

Manuscript received March, 1. T This research was supported by the Ministry of Education, Culture, Sports, Science and Technology of Japan through Grants-in-Aid for Scientific Research (No. 20246044, 19016004) and the Sasagawa Scientific Research Grant from The Japan Science Society.

Benoît Chapurlat is with Department of Bioengineering and Robotics, Tohoku University, Aoba-yama 01, Sendai-City 980-8579, Japan (e-mail: benoit@imech.mech.tohoku.ac.jp).

Hisataka Maruyama is with Department of Bioengineering and Robotics, Tohoku University, Aoba-yama 01, Sendai-City 980-8579, Japan (e-mail: maruyama@imech.mech.tohoku.ac.jp)

Yoko Yamanishi is with Department of Bioengineering and Robotics, Tohoku University, Aoba-yama 01, Sendai-City 980-8579, Japan (e-mail: yoko@imech.mech.tohoku.ac.jp)

Fumihito Arai was with Department of Bioengineering and Robotics, Tohoku University, Aoba-yama 01, Sendai-City 980-8579, Japan (e-mail: arai@imech.mech.tohoku.ac.jp).

II. First Filtration Process: Row of Microchannels

The sorting method chosen here consists of using rows of microchannels, the size of which would decide whether the beads pass or are blocked. Fig. 2 shows the gel microbead classification process. Two microfilters, for which the gap of the filter is different, are used for size classification. First, a sample solution including gel microbeads is injected into filter 1, which has a gap larger than that of filter 2, as shown in Fig. 2(a). Only beads with a diameter smaller than the channel width pass through. Gel microbeads passing through filter 1 are extracted and injected into filter 2 to remove those smaller than the gap of filter 2, as shown in Fig. 2(b). Finally, the stacked beads are extracted, as shown in Fig. 2(c). The size distribution of the separated gel microbeads is from the gap size of filter 2 to that of filter 1. Another possible method would be to filter the beads before exposing them to UV light for the crosslinking reaction. Gel beads are deformable as long as they are not exposed to UV light for a few minutes. In this case, the beads can pass through a channel of which's width is smaller than the diameter. However, if beads are not hardened by UV light just after passing the filter, they might combine with each other to form bigger beads, making the filtration useless. Because it is easier to solidify the beads during production rather than during filtration, we manipulated only beads that were already hardened.

We fabricated a PDMS microchannel microfilter by conventional photolithography and the replica molding method. We used SU-8 sheets 15 μm thick. The only tricky point during the fabrication process was to unmold the PDMS chip without tearing the PDMS channels. During unmolding, we poured ethanol between the mold and the chip to make unmolding easier. Omitting this step damages the mold. If PDMS is stuck in the mask, it is impossible to remove, and the mold becomes useless. The gap sizes chosen for filters 1 and 2 are 3.5 μm and 3.0 μm, respectively. Fig. 3 shows experimental results of size-dependent particle classification using a PDMS microfilter with a 3.5 μm gap. We separated gel microbeads smaller than 3.5 μm using the microfilter. Fig. 4 compares the particle size distribution before and after filtration. Before filtration, particle size was distributed from 2 μm to 10 μm. After filtration, all beads smaller than 3.5 μm had been eliminated, as shown in Fig. 4. We tried to use two-step filtration as explained in Fig. 2, but it was very difficult to recover beads after reflow of the second filter.

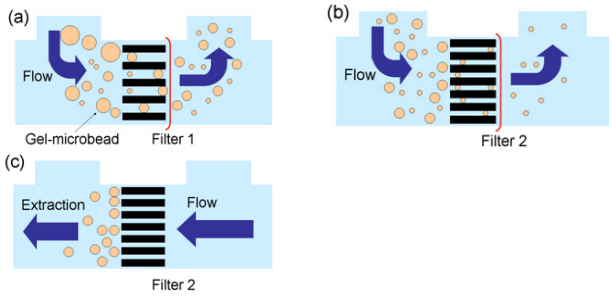

Fig. 2. Schematic of size-dependent classification of particles.

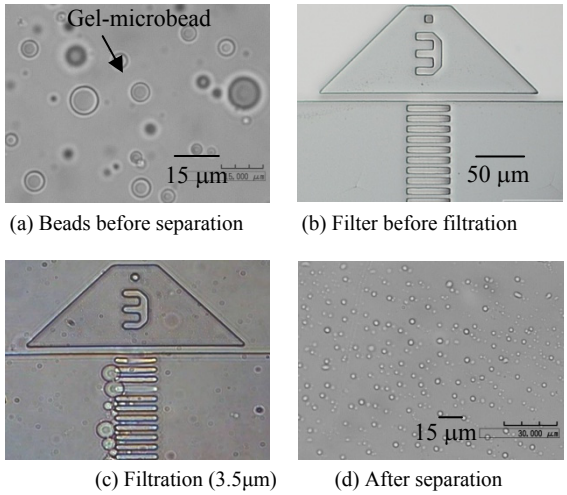

(a) Beads before separation (b) Filter before filtration

(c) Filtration (3.5μm) (d) After separation

Fig. 3. Experimental result of size-dependent particle classification using PDMS microfilter.

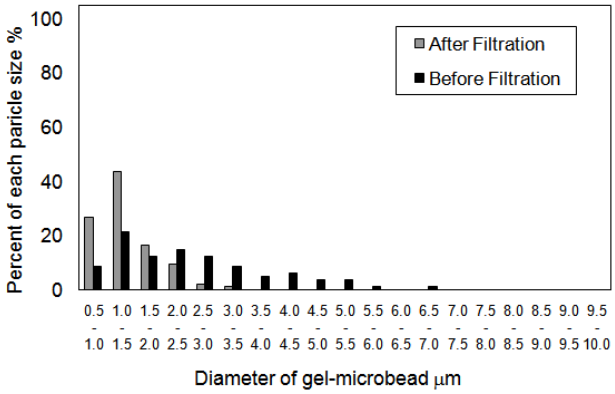

Fig. 4. Comparison of distribution of the particle size between before and after filtration with microchannel filter.

III. Second Filtration Process: Centrifugal Filter with Three-Dimensional MMT

A. Theory of grayscale

KMPR-1050 photoresist (Kayaku MicroChem Co., Ltd), the thick-film photoresist we used for the production of the MMT, is most sensitive to UV light at a wavelength of approximately 365 nm. The UV–optical absorptance of photoresists generally changes with the wavelength. In the case of multiple emitted wavelengths, the effectiveness of each is mixed, resulting in complex phenomena. For example, the complex relationship between exposure dose and cured depth can lead to the appearance of exposed and unexposed areas. As a result, we run the risk of having unexposed areas on the substrate.

In the present study, we cover a mercury lamp with a band-pass filter that has a peak at a wavelength of 365 nm to limit the bandwidth, and then we perform the exposure. The mercury lamp covered with the filter has an exposure dose of 15.4 [mJ/cm2]. If we consider that the thick KMPR

photoresist is a photosensitive resin, there is a relational expression between the amount of UV light and the cured depth, which is detailed below. Considering Eo [mJ/cm2] as the radiant energy per unit area, the exposure dose is expressed as a function of the cured depth *z* [mm] as follows. (Lambert–Beer's law) [10].

$$E(z) = E0 \square exp(-z/D) \quad (1)$$

D [mm], the depth at which UV energy is reduced to a 1/e fraction of the energy at the surface, is a characteristic of the resist. Supposing that *Ec* [mJ/cm2] is the critical value for exposure dose, it is related to the corresponding depth *Gd* [mm] at which the amount of exposure *E* reaches this value by the relation below.

$$Ec = E0 \square exp(-Gd/D) \quad (2)$$
$$Gd = D \square ln(E0/Ec) \quad (3)$$

Here, *Gd* is the cured depth corresponding to a radiant energy of *Eo*, *D* is the penetration depth of light, and *Ec* is the critical value for exposure dose.

B. Calibration of grayscale

Grayscale calibration is extremely important for precise control of the cured depth of the photoresist. In general, the gray pattern on the mask consists of a density of black dots.The average size of each dot on a high-precision imagesetter film is about 60 μm, which is bigger than the precision of the exposure machine (about 20 μm). This precision is not good enough to render the aggregation of black dots of the gray pattern. Therefore, in the present study, we used a 1/20 scale reduction projector to transcribe the film mask on an emulsion glass. The size of dots on the top of the mask is below the resolution of the exposure machine, so the machine sees only the average of the black dots' density and recognizes it as a uniform grayscale pattern.

By a spin-coating method, we placed a KMPR photoresist on 3 cm × 3 cm glass (thickness 120 μm) and then exposed it on the back side (1300 doses) and measured the cured depth using a profiler (KLA-Tencor). Fig. 5 shows the state of the resist observed after exposure of a mask calibrated with 256 shades of gray. Where the gray is at 70–75%, a sudden change was observed. When the UV exposure dose is high, the amount of cured resist grows. At that time, the number UV photons that were not absorbed by the resist increases, and finally the UV enter penetrate the resist, which becomes saturated. This phenomenon can be expressed through equation (3), which relates the exposure dose E and the cured depth Gd. Fig. 6 shows the relationship between the UV lamp power, calculated using the amount of light transmitted, and the cured depth. It is possible to design a grayscale mask by extracting an accurate cured depth of KMPR from this calibration curve.

C. Production of three-dimensional MMT using grayscale

Fig.8 shows the fabrication process of a 3 dimensional magnetic tool. We first spin coat some KMPR resist on a glass substrate (120 μm), then use UV to realize patterning. But this time, it is necessary to do a backside exposure, so that the part of the KMPR negative resist first exposed, the one which hardens first, is the one in contact with the glass substrate. Then, with the same process than 2 dimensional MMT, we coat using a mix of PDMS and magnetite (50w% of Fe3O4) and, after the bake (80 Celsius degrees), we use a striper liquid to remove the completed 3 dimensional magnetic tool. Fig.7 displays the 3 dimensional MMT complex shapes obtained using the KMPR mold. Fig. 9 shows the mold sculpted in the KMPR on the top of the glass substrate by grayscale technique. The 3 dimensional MMT presents a maximum difference of height around 110 μm, and we confirmed that it is possible to produce a microtool with smooth curves in only one exposure step.

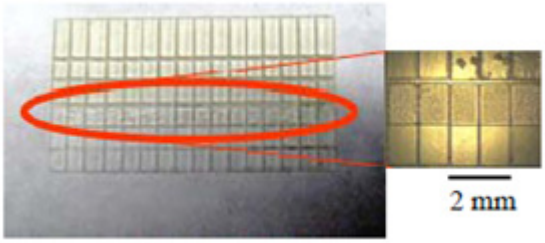

Fig. 5: Patterned KMPR photoresist for calibration

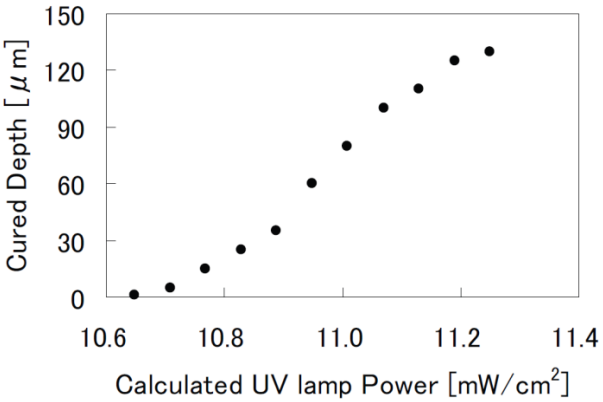

Fig.6: Calibration curve of the grey-scale photolithography (with Bandpass Filter at 365nm)

Fig.7: Three-dimensional patterning of KMPR

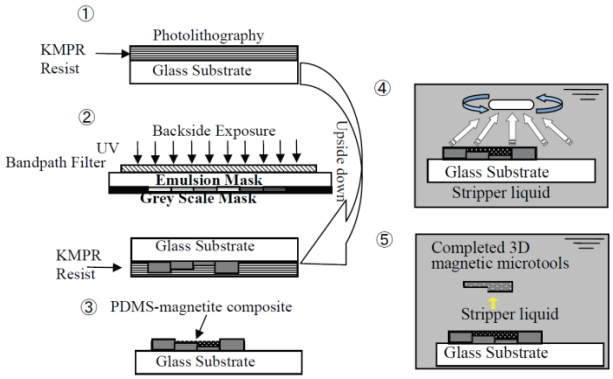

Fig.8: Fabrication processs of 3D-MMT

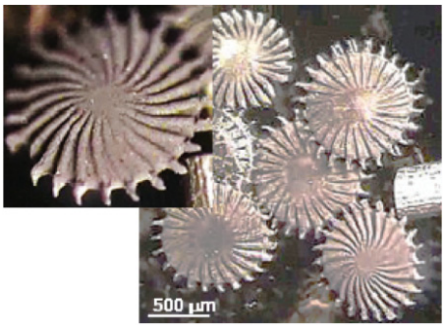

Fig. 9: Gear-shaped 3D-MMT

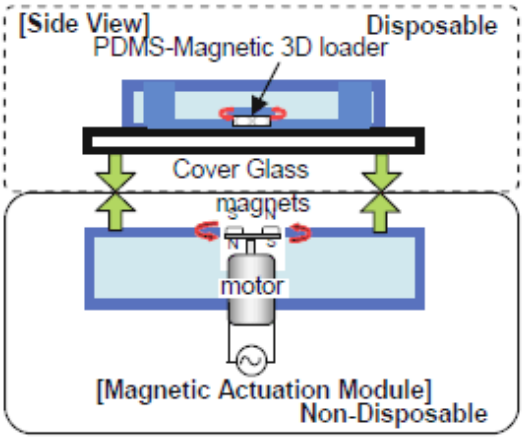

Fig. 10: Actuation module of filtration system

D. 3D MMT for Filtration

Among other possible applications of the 3D-MMT rotating mechanism, it is possible to build filtration systems [11, 12]. Fig 11 shows the result of numerical simulation of the distribution of velocity around the rotating 2D (Flat) and 3D (Tapered)-MMT. 3D MMT can generate force toward outside by swelling flow. Fig. 12 presents the basic concept of a chip for sorting particles of several sizes using rotational flow. The chamber in which the 3D-MMT rotor was inserted has a height greater than h, the height of the filtration gate. Beads with a diameter less than h are evacuated to the external channel because of the rotational flow. This time the 3D-MMT we use is driven by a system similar to that shown in Fig. 10, but to reach high rotation speeds (with a maximum rotation speed around 4000 rpm), we use a DC motor rather than a stepping motor. We fix symmetrically a pair of permanent magnets on a disc centered on the central axis of the motor. This method was first tested with a large-scale filter with h = 50 µm and using beads of 50 and 100 µm. As the separation appeared to be efficient, we applied this technique to filtration of 3.5 µm beads.

The fabrication process of the filtration chip is presented Fig. 13. The first layer is used to fabricate pillars which would prevent the cellar of filtration area to stick on the glass. The second layer is used for the inner and outer chambers. First, a mixture of SU-8 3050 and ethanol (2:1) is spin-coated at 3000 rpm for 30 s to obtain a thickness around 3.5 µm. After a 100-dose exposure, a 50 µm SU-8 sheet is fastened on top and later exposed with 200 doses.

When realizing the chip, one particular point has to be considered. To increase the height of the inner chamber, the stick a PDMS cylinder on the mold (diameter 5 mm, height 3 mm). It is indispensable to put plasma on the cylinder before attaching it to the mold. This prevents the PDMS of the chip and the cylinder from uniting and allows easy unmolding. The rest of the process is easy, as it does not differ from conventional chip fabrication.

This filter was then used for bead separation using the same bead sample we used for the previous method. With this rotational flow filtration mechanism, even when big beads are trapped in the filtration gate, they continue moving and follow the current in the inner chamber because of the flow created by the MMT's rotating mechanism. Thus, the filter is not blocked, making it possible to filter the beads continuously no matter how long it takes. Beads would not get stuck in the filter as easily as they used to with the microchannel version. We can see in Fig. 14 that big beads stay at the limit of the filter in the inner chamber, and little ones pass through. The filter exhibits good filtering properties, as shown in the size distribution in Fig. 15.

This method offers an advantage regarding adaptability to different filtration sizes. For the first method (channel filtration), the width of the channel must be decided during CAD file design. Changing the width involves restarting the whole process from the fabrication of the mask. In contrast, with the second method, the height of the filtration area is determined by the parameter chosen for the first layer of SU-8 coated on the silicon wafer.

However, because the size of the microchannel for the first filter does not depend on the fabrication process, we are sure about obtaining the same results after every fabrication. With the rotational filter, experiments fix the height of the filter. Two consecutive spin-coatings will not yield perfectly similar results. Therefore, it is necessary to measure every sample to determine whether it meets the required target size. The problem of the microchannel filter has been partially solved, and quick clogging of the filter is avoided.

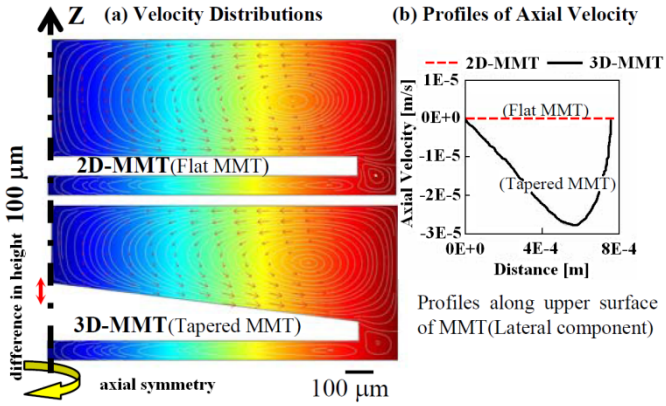

Fig. 11: Distribution of velocity around the rotating 2D (Flat) and 3D (Tapered)-MMT. (a) Velocity distribution, (b) Profiles of axial velocity along the lateral component.

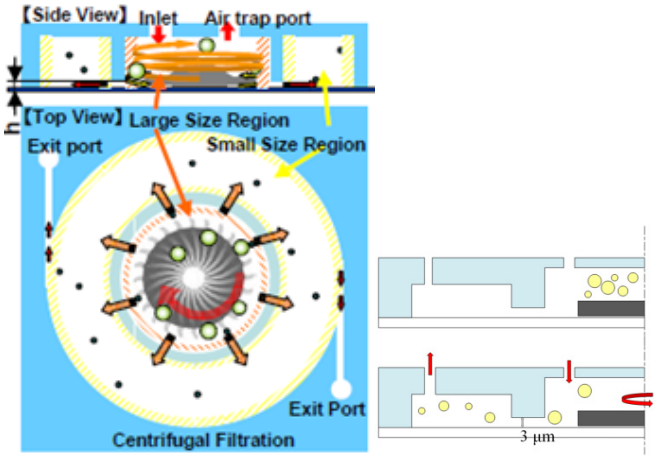

Fig. 12: Concept of on-chip centrifugal filtration by 3D-MMT

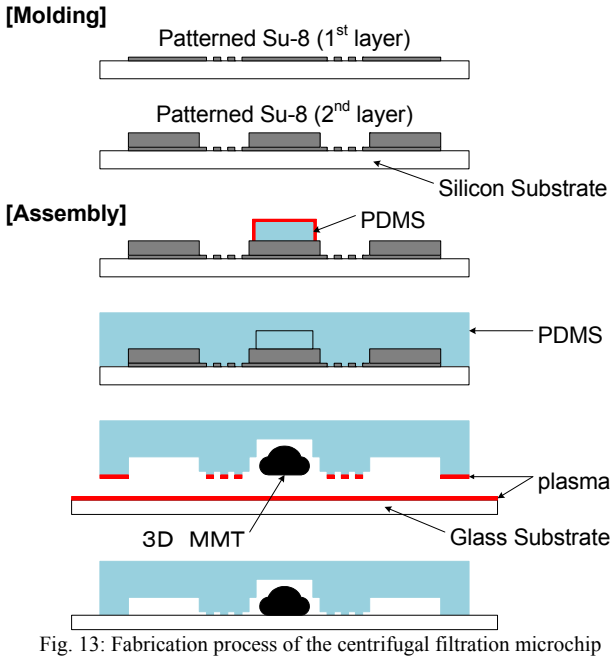

Fig. 13: Fabrication process of the centrifugal filtration microchip

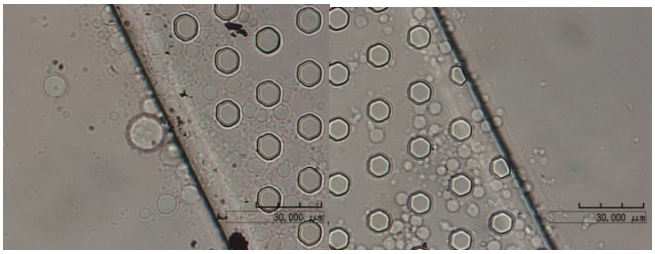

Fig. 14: Results of the filtration with rotational filter (left: inner chamber; right: outer chamber).

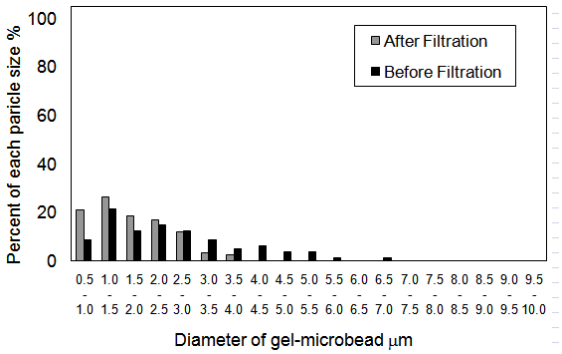

Fig.15: Comparison of distribution of the particle size between before and after filtration with microchannel filter.

E. Alternative filtration method

In order to have a filter which allows continuous filtration, we developed another type of filter, although not applied already at a scale of few microns [13]. This filter has a spiral shaped main channel linked to a central chamber in which is included a rotor microtool. The rotor creates a flow from the central chamber to the output through the main channel. Along the main channel, we fabricate a parallel channel separated from the main channel by a filtration area such as the one used previously. Because of centrifugal force, part of the little beads will go through this filtration area and go to the parallel channel (Fig.16). The mask for this microchip is produced using a 3 steps exposure process, using SU-8 sheets. Each microchannel is 200 μm in wide and 128 μm in deep. Width of sidewall is 100 μm and the height of filters is 24 μm for inner one and 58 μm for the outer one. Then we used beads of 20, 50 and 70 μm polystyrene beads to verify the filtration properties of the filter, as shown in Fig. 17.

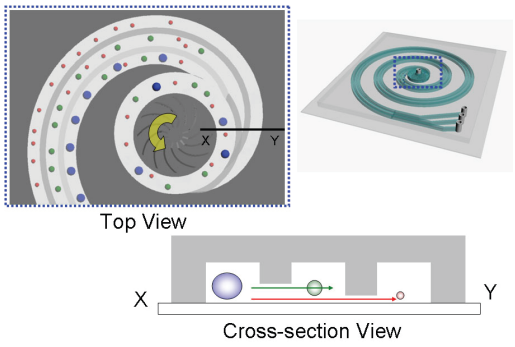

Fig.16: Principle of the spiral-shaped filter.

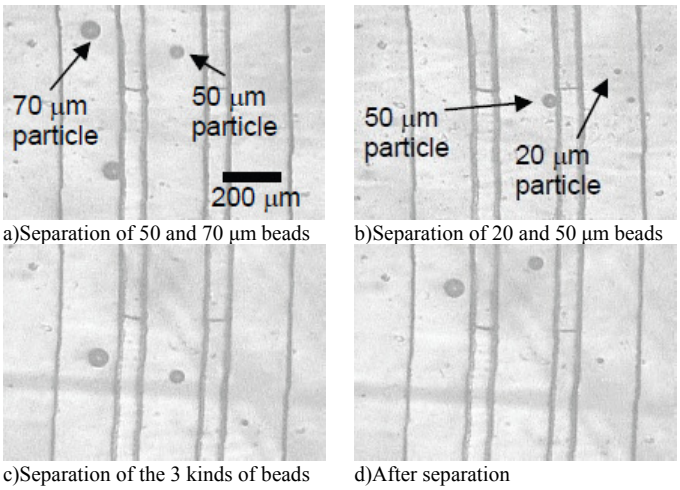

a)Separation of 50 and 70 µm beads b)Separation of 20 and 50 µm beads

c)Separation of the 3 kinds of beads d)After separation

Fig.17: Experimental result of particle filtering

IV. PRODUCTION OF FUNCTIONAL MICROTOOLS

After we were able to isolate gel beads of the same size using the filtration devices detailed above, our next goal was to use those beads to fabricate tether-shaped gel tools. When we use a 3.4 wt% dipotassium phosphate dipotassium salt solution, we can connect gel microbeads to each other under UV illumination.

The manipulation of the gel beads is realized with optical tweezers manipulated with a joystick [14]. The gel beads can stick to the glass, and the tweezers' force is not big enough to detach them. Thus, it is first necessary to connect the first beads vertically to move the tip of the gel tool away from the glass to prevent the tip from sticking to the glass.

Once the first beads are connected, we connect the next beads laterally to build what would be the functional part of the gel tool. After the beads have been connected, we can move the gel bid on the tip and then manipulate the whole chain.

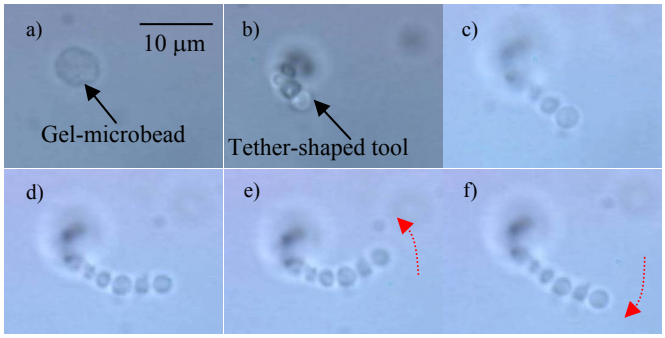

Fig. 18 Production of the tether-shaped gel-tool using separated gel-microbeads: (a) gel-microbead, (b) –(c)construction of the tool, (d) tether-shaped tool, (e), (f)bending of tethered-tool

V. CONCLUSIONS

As we faced a size regulation issue, we had to find a method to homogenize the size of gel beads. The first method we used, involving a row of microchannels with a determined size, led to good results with a size repartition suitable for microtool fabrication. However, this method had several drawbacks, such as clogging of the channels or deterioration of the filter.

In the second proposed method, we use centrifugal force to separate little beads from big ones. This process is realized without the filter getting stuck, which means a single chip could be used for several filtrations. We also began developing a new continuous filtration method using a spiral-shaped channel.

Finally, we manipulated size-classified gel microbeads and fabricated a tether-shaped gel tool. Ten gel microbeads were connected by contact under UV illumination in a phosphate dipotassium salt solution. Production of a functional microtool with size-classified gel microbeads was achieved.

ACKNOWLEDGMENT

This research was supported by the Ministry of Education, Culture, Sports, Science and Technology of Japan through Grants-in-Aid for Scientific Research (No. 20246044, 19016004) and the Sasagawa Scientific Research Grant from The Japan Science Society.

REFERENCES

[1] Maruyama, H., Arai F. & Fukuda T., "On-Chip pH Measurement Using Functionalized Gel-Microbeads Positioned by Optical Tweezers", Lab Chip, 7, 346-351 (2008)

[2] Maruyama, H., Arai F. & Fukuda T., Proc of ICRA2008, pp. 305-310 (2008)

[3] M. Yamada, M. Nakashima, & M. Seki, "Pinched Flow Fractionation: Continuous Size Separation of Particles Utilizing a Laminar Flow Profile in a Pinched Microchannel", Anal. Chem, 76, pp. 5465-5471 (2004)

[4] M. Yamada & M. Seki, "Microfluidic Particle Sorter Employing Flow Splitting and Recombining", Anal. Chem., 78, pp. 1357-1362 (2006)

[5] J. Takagi, M. Yamada, M. Yasuda & M. Seki, "Continuous particle separation in a microchannel having asymmetrically arranged multiple branches", Lab Chip, 5, pp. 778–784 (2005)

[6] M. Yamada & M. Seki, "Hydrodynamic filtration for on-chip particle concentration and classification utilizing microfluidics", Lab Chip, 5, pp. 1233–1239 (2005)

[7] C. Lay, et. al, s"Enhanced microfiltration devices configured with hydrodynamic trapping and a rain drop bypass filtering architecture for microbial cells detection", Lab Chip 8, pp.830-833 (2008)

[8] D. Mc Gloin, "Optical tweezers: 20 years on", Phil. Trans. R. Soc. A, 364, pp.3521-3537 (2006)

[9] A. Ashkin, "Optical trapping an manipulation of neutral particles using lasers", Peoc. Natl. Acad.Sci USA. Vol 94, pp 4853-4860 (1997)

[10] Paul F. Jacobs, "Rapid Prototyping & Manufacturing – Fundamentals of StereoLithography", Society of Manufacturing Engineers, Ch.2, 1992

[11] Y. Yamanishi, S. Sakuma, K. Onda & F. Arai, "Biocompatible polymeric magnetically driven microtool for particle sorting", Journal of Micro-Nano Mechatronics, (2008)

[12] Y. Yamanishi, Y.C. Lin & F. Arai, "Magnetically Modified PDMS Devices for Active Microfluidic Control", u-TAS2007, p.883-885, (2007).

[13] H. Maruyama, S. Sakuma, Y. Yamanishi and F. Arai, SIZE-DEPENDENT PARTICLE FILTERATION USING MAGNETICALLY DRIVEN MICROTOOL AND CENTRIFUGAL FORCE IN MICROCHIP, Proc. of MEMS2009, pp. 375-378 (2009)

[14] F. Arai, K. Yoshikawa, T. Sakami & T. Fukuda: "Synchronized laser micromanipulation of multiple targets along each trajectory by single laser", Applied Physics Letters, 85, 19, pp. 4301-4303 (2004).